Elucidation of molecular dynamics by X-ray transient-absorption spectroscopy

Valeriu Scutelnic and Stephen R. Leone

Departments of Chemistry and Physics, University of California, and Lawrence Berkeley National Laboratory, Berkeley, CA 94720

X-ray absorption spectroscopy on attosecond and femtosecond timescales is a frontier of modern ultrafast science. For the last two decades, ultrafast lasers produced ever growing powers that facilitate implementation of attosecond high-harmonic X-ray sources in compact equipment. This unique broad-band light source opens the door for numerous applications; in particular it is ideal for chemical dynamics studies due to its sensitivity to electronic and vibrational state changes. Here, we outline briefly the evolution of time-resolved technology and review several case studies in which extreme ultraviolet and soft X-ray spectroscopy prove its exclusive sensitivity to the electronic structure of molecular species.

1 Introduction

Photochemistry is of paramount importance for understanding biological processes (*e.g.* formation of vitamin D, photosynthesis, and vision),[1–3] atmospheric light-induced transformations[4,5] and the engineering of more efficient solar cells.[6,7] Photochemical reactions, unlike thermally controlled reactions, often proceed through multiple pathways, which lead to a rich variety of possible mechanisms. Our modern understanding of such processes has been shaped significantly by advances in experimental methods. The latest push in this exciting realm is ultrafast X-ray spectroscopy. First, we give a brief description of the historical premises that brought about the powerful attosecond and femtosecond X-ray technology available today.

The last century observed a vertiginous technological ascend giving access to ever shorter timescales. The first attempt to measure rates of chemical reactions down to millisecond resolution was done by H. Hartridge and F. J. W. Roughton (1923) with fast mixing of the reagents.[8] Two decades later, Norrish and Porter ingeniously applied

gas-discharge flash-lamps, which were initially invented for photography, to trigger chemical reactions.[9] This laid the basis for flash photolysis and relaxation methods and gave access to intermediates with microsecond lifetimes.[10] Undoubtedly, the first laser engineered by Theodore Maiman in 1960 initiated a new era in experimental physical chemistry,[11] as the next years witnessed the realization of a cornucopia of applications. Among those, the most significant for ultrafast science are the Q-switching technique, discovered by Hellwarth in 1961 using the Kerr effect that shortened the laser pulse duration to nanoseconds,[12] and mode-locking (DeMaria, 1966)[13] that ultimately achieved femtosecond resolution (colliding pulse mode-locking invented in 1980 by Richard Fork *et al.* produced <100 fs pulses).[14]

In a series of seminal works, Zewail applied the femtosecond laser technology to observations of chemical dynamics at the intrinsic timescale of the molecular vibration, which gave birth to the field of femtochemistry.[15] As a result, a family of techniques have been elaborated to probe coherences in the visible,[16] and later in the infrared (IR)[17] and ultraviolet (UV) range.[18–20] By the end of the 1980s, laser pulses from dye lasers could be compressed to a few femtoseconds[21] and further amplified to high powers with chirped-pulse amplification (CPA).[22] The intense laser field rendered possible the discovery of high-order harmonic generation (HHG) in gases by McPherson *et al.* (1987).[23] Further augmented by the development of short pulse lasers based on Nd and Ti ions in solid-state materials, this gave the unprecedented capability to generate extreme ultraviolet (XUV) and soft X-ray pulses with few-femtosecond to attosecond duration in table-top setups.

Ultrafast X-ray science also benefited from a parallel development at accelerator facilities. Since the 1970s, synchrotron light sources paved the way for the application of X-ray absorption spectroscopy in a pump-probe fashion.[24] The synchrotron pulses were limited initially to 10-100 ps.[25,26] With a pulse slicing technique, implemented at the Advanced Light Source (ALS) by Zolotorev and coworkers,[27] it became feasible to extract femtosecond pulses from the storage rings. In the last decade, several X-ray free electron lasers have been constructed that provide intense few-fs pulses.[28]

Nowadays, pump-probe X-ray spectroscopy flourishes with numerous applications across various fields. In the present contribution, we discuss state-of-the-art HHG-based X-ray (and XUV) transient-absorption spectroscopy and the recent achievements in molecular dynamics.

2 High-harmonic extreme ultraviolet probe

X-rays are a highly versatile spectroscopic tool thanks to their ability to excite electrons from the core to valence orbitals, which leads to element specificity (the core orbital energy is distinct for each element, see Figure 1a), charge and chemical bonding sensitivity, providing an exceptional insight into the nature of electronic transformations.[29,30] In contrast to the multiphoton probing with optical pulses (e.g. multiphoton ionization), one X-ray photon is involved in the core-to-valence transition, thus relaxing the requirement and complexity of intermediate resonances.

High-order harmonic generation, or HHG, is the emission of odd harmonics at the non-perturbative interaction of an intense laser pulse with a target material such as an atom. This process is a strong-field phenomenon and is qualitatively described by a semiclassical picture of the three-step model, depicted in Figure 1b.[31–34] First, the electric field of the intense pulse distorts the Coulomb potential of the atom, such that

an electron tunnels through the barrier and leaves the ion residue behind. Second, the electron wave packet is accelerated and, once the electric field switches, the electron is directed back to the ionized atom. Third, in the subsequent recombination a high energy photon is emitted. This photon is in phase with the driving laser field and has the same polarization. Moreover, since the recombination occurs only in a small fraction of the optical cycle, the emitted high-harmonic pulse is shorter than the driving laser pulse and can reach attosecond duration. In the spectral range, the harmonics extend up to a cutoff energy $E_{cutoff} = 3.17 \cdot U_p + I_p$, where U_p is the ponderomotive energy of the electron and I_p is the ionization potential of the atom. U_p scales quadratically with the optical wavelength, and depending on the laser wavelength employed, the high harmonics can cover the XUV and soft X-ray spectral ranges.

A popular method for observing molecular transformations in real time is by triggering the dynamics with a short pump pulse and interrogating, after a defined delay, the return of the system to equilibrium with a broadband probe pulse that is subsequently spectrally dispersed (Figure 1c). Broadband HHG pulses are an excellent candidate for utilization in a pump-probe scheme. In a landmark experiment, the groups at UC Berkeley and Munich developed the method of attosecond transient-absorption spectroscopy (ATAS), which allowed them to track directly the electron wave-packet motion in krypton cation.[35] ATAS offers both time and spectral resolution by resolving spectrally the attosecond pulse after the interaction with sample – because the probe pulse is not time-resolved, the width of spectral bands are limited by the lifetime of the induced polarization in the sample.[36] In this sense, the time–energy uncertainty limitation is circumvented.

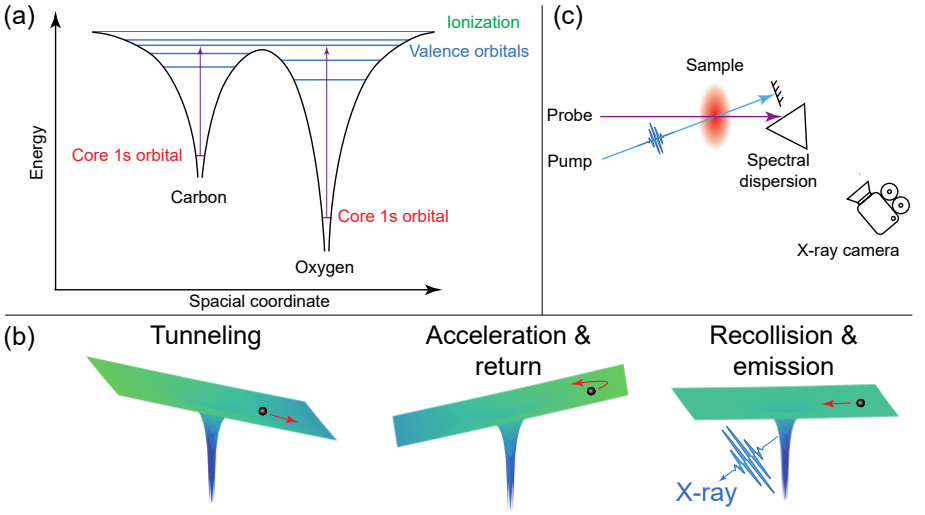

Figure 1. (a) Energy diagram of a heteronuclear diatomic molecule – carbon monoxide,[37,38] core orbitals (red) are localized at the nuclei, while the valence orbitals (blue) pertain to the entire molecule. Purple arrows represent transitions from carbon and oxygen cores to a vacant valence orbital. **(b)** In the HHG process, the atomic potential well is distorted in the oscillating electric field, an electron wave packet tunnels through the barrier, is accelerated and recombines with the ion, emitting a highly energetic photon.[32] **(c)** Pump-probe scheme with spectral dispersion of the

probe pulse onto a camera. Pump-probe angles near zero degrees are chosen for best time resolution.

Nowadays, CPA pulses are routinely used to generate high harmonics in the XUV (10-100 eV pulses covering the absorption edges of various heavy elements), and, in combination with various optical gating schemes, isolated attosecond pulses are consistently produced.[39–42] Spectroscopy with ultra-broadband HHG pulses is the method of choice for probing the coupling of nuclear and electronic dynamics. In the following examples, bromine and iodine serve as reporter atoms of attosecond molecular dynamics in XUV transient-absorption experiments.

The Born-Oppenheimer approximation breaks down when electronic states approach in energy, and the direct observation of the electronic character change has been a tantalizing task in the ultrafast field.[43] One such example is the conical intersection between the $^1Q_1$ and $^3Q_{0+}$ states in CH_3Br. Triggering a valence excited state with an intense few-fs IR pulse and probing the bromine $M_{4,5}$ edge allowed Timmers *et al.* to successfully monitor the non-adiabatic population transfer in CH_3Br. ATAS exhibits a clear signature of the valence excited state wave packet and its bifurcation from the initial excitation to the conical intersection and to the ensuing dissociation (channel 1 in Figure 2). Apart from this, vibrational and electronic coherences in CH_3Br (channels 2 and 3 in Figure 2) initiated by strong-field excitation are spectrally well resolved from the valence dynamics, thus validating the potential of ATAS to track simultaneously different processes.[44] In an analogous system, CH_3I, the group of Zhi-Heng Loh distinguished C-I stretch and CH_3 umbrella modes of coherent vibrational superpositions launched by strong-field ionization initiated through a bond-softening mechanism.[45]

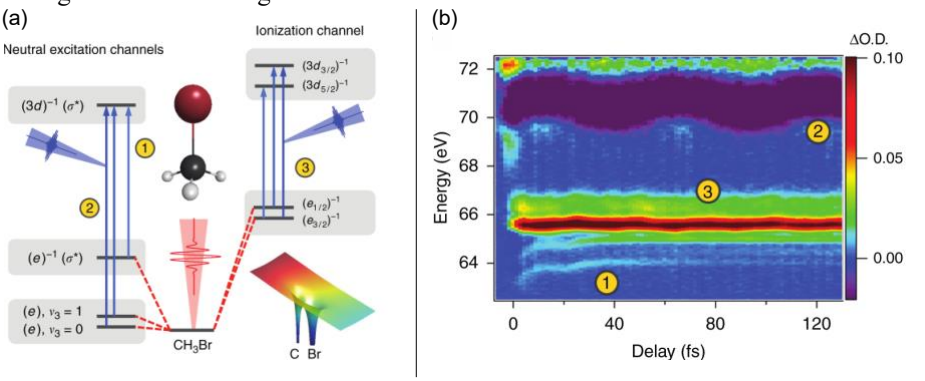

Figure 2. (a) Energy diagram of CH_3Br. **(b)** Attosecond transient-absorption spectroscopy of CH_3Br. Three channels are resolved: (1) neutral excited-state wave packet, (2) ground-state vibrational wave packet, (3) ionic spin-orbit coupled wave packet. (Reproduced from ref. 44 under the Creative Commons license.)

Likewise, ATAS readily senses the electronic and vibrational coherences prepared by an intense IR pulse in deuterium bromide. Kobayashi *et al.* reported on identification and characterization of electronic and vibrational coherences in the ionic DBr^+ by means of bromine 3*d* core-level absorption spectra.[46] Electronic coherences occur with a period of 12.6 fs, corresponding to the $X\,^2\Pi_{3/2}$ and $X\,^2\Pi_{1/2}$ states of HBr^+, and vibrational coherences have a period of 19.9 fs (Figure 3). A clear difference is

observed in the behavior of the electronic and vibrational coherences: the former shows dependence on the relative polarization of the pump and probe pulses and partially decays on a 100-fs timescale due to rotational decoherence, while the latter is largely independent of the pump/probe polarization and maintains a nearly constant amplitude in the measured time window.

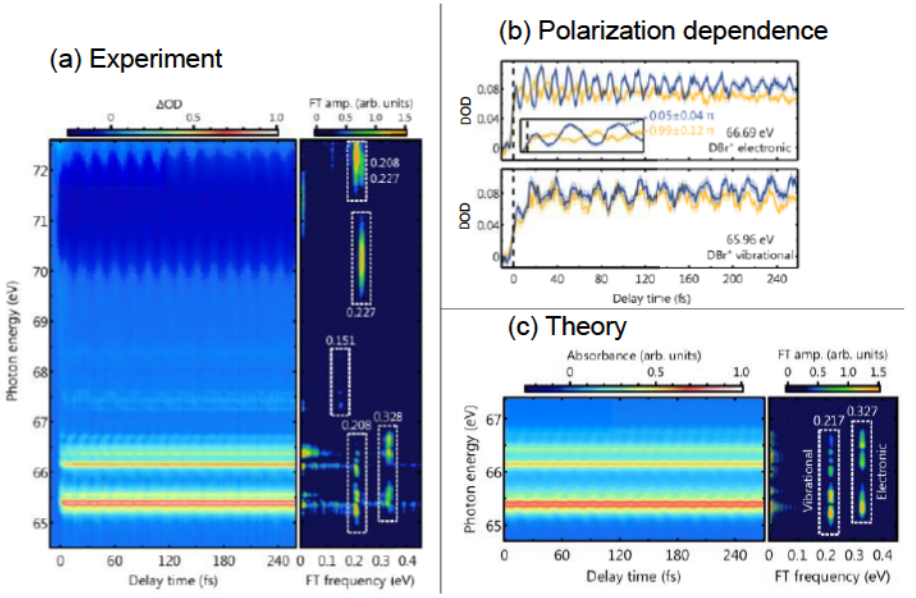

Figure 3. (a) Left: Experimental delay-dependent ATAS spectra of strong-field excited DBr. Right: Fourier transform of the experimental spectra along the delay axis, the numbers indicating the beat frequencies in units of eV. **(b)** Comparison between the parallel polarization (blue) and the perpendicular polarization (yellow) of pump and probe. The inset is a zoom of the early-time electronic quantum beats. Quantum beats originating from the vibrational coherences are identical between the two polarization measurements, whereas those originating from the electronic coherence show clear contrast. **(c)** Left: Simulated delay-dependent ATAS spectra for the coherently prepared $X\,^2\Pi_{3/2}$ and $X\,^2\Pi_{1/2}$ states of HBr^+. Right: Fourier transform of the simulated spectra along the delay axis. (Adapted with permission from ref. 46, copyright 2020 American Physical Society.)

Passage through an avoided crossing was monitored in fascinating detail in the example of the diatomic molecule IBr (Kobayashi *et al.*).[47] A 8-fs optical pulse was employed to resonantly excite the $B(^3\Pi_{0+})$ state in the vicinity of the curve crossing between $B(^3\Pi_{0+})$ and $Y(0^+)$ states (Figure 4a). Both atoms were tracked concomitantly through iodine 4*d* and bromine 3*d* transitions to valence orbitals. Massive changes in core-to-valence transition energies were observed in the first 100 fs, when the wave packet traverses the B/Y curve crossing as the bond length increases towards dissociation (Figure 4b). The dissociation on the $B(^3\Pi_{0+})$ potential is apparent in the time window of 0-50 fs. Later, rapid switching of the electronic character at the avoided crossing (50-80 fs) is vividly portrayed in the transient absorption XUV spectra of iodine and bromine.

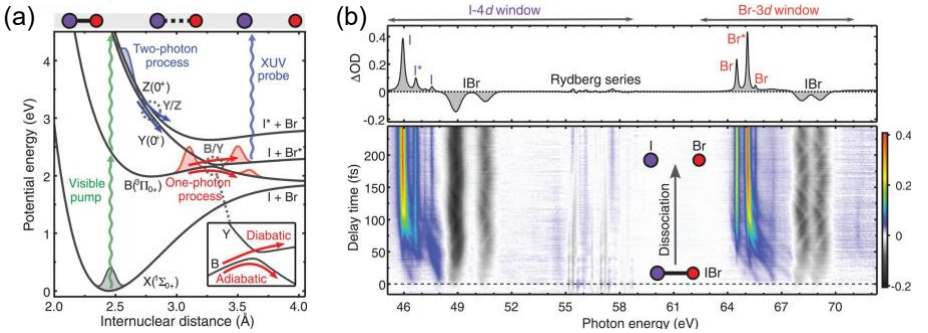

Figure 4. (a) Adiabatic potential energy curves of IBr. Visible and XUV photon excitations are indicated with vertical arrows. Red and blue wave packets represent dissociation from one- and two-photon excitation, respectively. Inset: zoom of the B/Y avoided crossing. **(b)** Top: Dissociation products are indicated in the transient absorption spectrum recorded at long delays. Bottom: Complete map of the time-resolved transient-absorption spectra recorded in the region of iodine $N_{4,5}$ and bromine $M_{4,5}$ edges, excited-state signal is shown in a bright color scale. (Adapted with permission from ref. 47, copyright 2019 AAAS.)

3 High-harmonic soft X-ray probe

Such biologically relevant elements as carbon, nitrogen, oxygen and sulfur absorb X-rays above 100 eV. For this reason, extending HHG to the soft X-ray range is an attractive avenue for further development of the XUV ATAS. Efficient up-conversion of IR photons into soft X-rays can be achieved by driving the HHG process with a longer wavelength IR pulse, as the maximum HHG photon energy scales quadratically with increasing wavelength.[48] A stepping stone towards ATAS in the soft X-ray range was achieved by Attar *et al.*, generating high harmonics in the soft X-ray range with the output of an optical parametric amplifier (50 fs pulse duration, centered at ~1300 nm).[49] HHG covering the carbon K-edge (at 285 eV) allowed Attar *et al.* to capture the key intermediate in the ring-opening of cyclohexadiene induced by UV light. Carbon 1*s* spectra underpinned the decay to the linear hexatriene through the pericyclic minimum, in which the frontier orbitals underwent strong mixing and overlapping. Similarly, Pertot *et al.* demonstrated the use of an 1800 nm wavelength driver pulse to generate X-ray flux at carbon K-edge – they tracked the course of dissociation after strong-field ionization of SF_6 and CF_4 and the splitting of absorption bands due to symmetry breaking.[30]

The sensitivity of soft X-ray transient-absorption spectroscopy to changes in molecular structure and orbital occupancy was proven in the example of benzene radical cation (Bz^+) by Epshtein *et al.*[50] The ground state of Bz^+ was prepared selectively through resonance enhanced multiple photon ionization REMPI by excitation with two 267 nm photons. Comparison of the X-ray absorption spectra of the neutral benzene and the benzene radical cation (Figure 5) shows a splitting of the two degenerate π* orbitals (peak A, and peaks F and G in Bz and Bz^+, respectively) as well as an appearance of a new peak (peak E) due to excitation to the partially occupied

π-subshell. High-level *ab initio* calculations[51] assign the π* orbital splitting of the cation (peaks F and G) to both the Jahn-Teller geometry distortion and spin coupling of the unpaired electron in the partially vacant π orbital with the unpaired electrons resulting from the $1s_C \rightarrow \pi^*$ transition. The spin coupling was calculated to be the major contribution to the observed splitting.

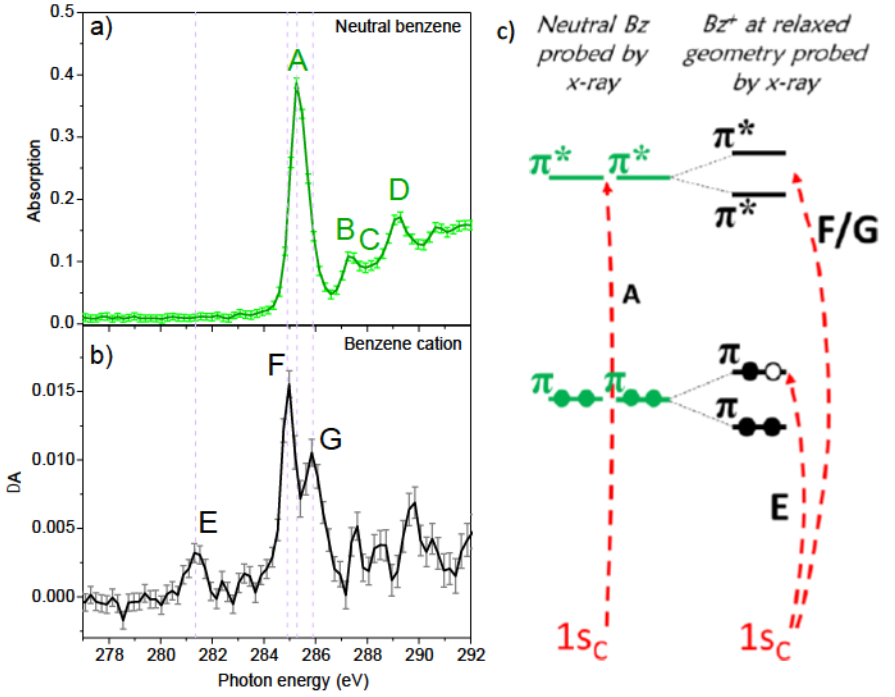

Figure 5. Soft X-ray absorption spectrum of the ground-state neutral benzene **(a)** and radical cation **(b)**. **(c)** Molecular orbital diagram illustrating the main transitions responsible for the spectral features in the cation (Bz = benzene). (Reprinted with permission from ref. 50. Copyright 2020 American Chemical Society.)

Soft X-ray transient absorption of photoexcited pyrazine unraveled the participation of the elusive optically dark ^1A_u ($n\pi^*$) state in deexcitation to the ground state (Figure 6).[52] The previously characterized $^1B_{2u}$ ($\pi\pi^*$) (S_2) and $^1B_{3u}$ ($n\pi^*$) (S_1) states are also distinguished. The spectral assignment was aided by a combination of electronic structure calculations and nonadiabatic dynamics simulations. The optically dark ^1A_u ($n\pi^*$) state, differing only slightly from the $^1B_{3u}$ ($n\pi^*$) state in minimum energy, is significantly different in core-to-valence transition energies and oscillator strengths. The ^1A_u ($n\pi^*$) state is populated about 200 femtoseconds after electronic excitation and plays a key role in the relaxation of pyrazine to the ground state. More examples of soft X-rays exquisite sensitivity to UV-induced ring-opening, intersystem crossing and radical formation dynamics can be found in the review by Bhattacherjee *et al.*[53]

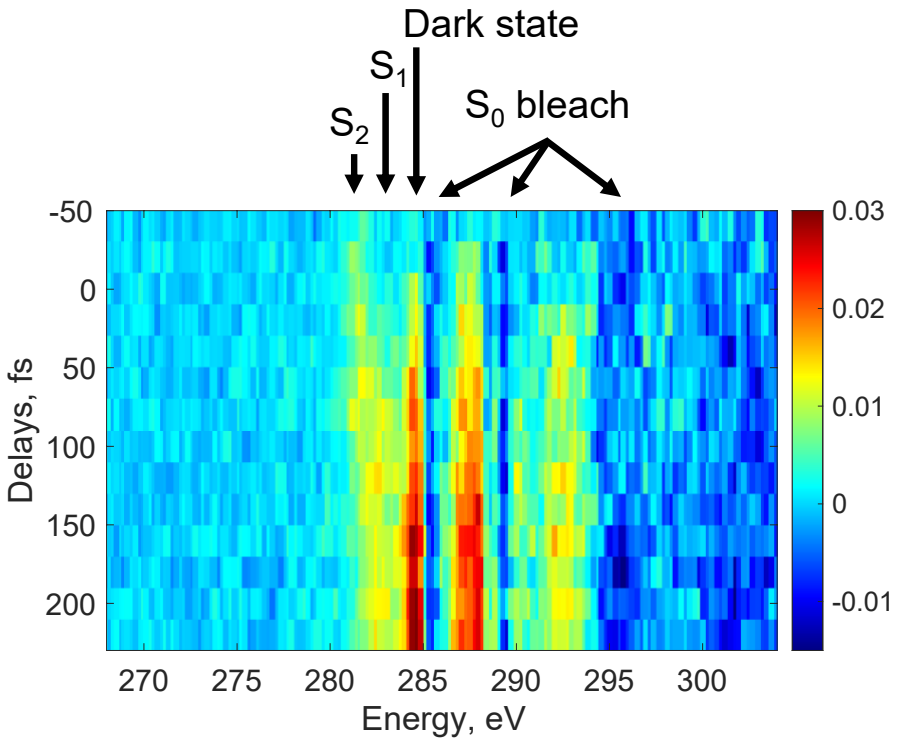

Figure 6. Two-dimensional map of the time-resolved transient-absorption spectra in dependence of the time delay between 267 nm pump and soft X-ray probe.

4 From femtosecond to attosecond X-ray probe

Currently, significant effort in the community is dedicated toward the synthesis of isolated attosecond pulses that cover larger and larger soft X-ray ranges and allow compressing the pulse duration to a few tens of attoseconds. The mid-IR laser sources developed for this purpose were covered in detail by X. Ren *et al*.[48] Here we refer to several of the latest strides in this direction that lead to sufficient fluxes for measurements. Li *et al.* utilized 1800 nm pulses of an optical parametric chirped-pulse amplifier (OPCPA) to obtain 53 attosecond pulses that extend out to 300 eV.[54] Compressing a pulse centered at 1600 nm with a large bandwidth allowed Gaumnitz *et al*. to obtain a record 43 attosecond pulse reaching 180 eV.[55] Keller and coworkers demonstrated the use of 2200-nm driver pulses from an OPCPA to produce harmonics up to 600 eV. A special differential pumping scheme was engineered to afford up to 70 bar gas pressure in the HHG cell, which was necessary for achieving phase matching.[56] Parallel research in Jon Marangos' group employed 1800 nm pulses of an optical parametric amplifier (OPA) to produce photons up to 600 eV.[57]

The increase of driver wavelength comes at the expense of the detrimental reduction of the HHG flux as $\sim\lambda_{laser}^{-6}$.[58] Barreau *et al.*[59] used the output of an OPA at 1300 nm, which is spectrally broadened in a hollow-core fiber and then compressed with custom chirped mirrors. 1300 nm wavelength is chosen to increase the photon energy cutoff to the carbon K-edge while maintaining a high flux. Broadband pulses

centered at 1300 nm measuring sub-13 fs in duration and attosecond X-ray pulses that cover up to 370 eV have been achieved.[59] It was demonstrated that this light source is suitable to measure high-quality absorption spectra at the carbon K-edge in a few seconds, sufficient to carry out pump-probe experiments with less than 11 fs temporal resolution, thus enabling studies of the nonadiabatic dynamics and topology at curve crossings[60] and conical intersections,[61–63] electronic wave packet dynamics.[64,65]

The technique holds great promise to resolve dynamics at an unprecedented level of detail in organic molecules, as suggested by the work of Zinchenko *et al.*[66] Strong-field ionization of ethylene to the lowest electronic excited state (D_1) of $C_2H_4^+$ was found to undergo electronic relaxation to the ground state (D_0) in less than 7 fs.[66] Such an efficient funneling of the electronic energy in less than a vibrational period is feasible due to the presence of a conical intersection with the ionic ground state that is reached in a very short time. In particular, the D_1 and D_0 states could be separately tracked because the $1s \rightarrow \pi^*$ transition from the D_1 state is ~1 eV redshifted from the corresponding transition from the D_0 state. The large shift is explained on the basis of the electron correlation of the unpaired spins, a similar spin-coupling effect was observed in the core-to-valence excitation of the benzene radical cation, N_2^+, CO^+, and NH_3^+.[51,67–69] This is another eloquent example of electronic structure selectivity of the X-rays.

In conclusion, we have considered the historic context of the ultrafast science, and analyzed examples of applications to chemical dynamics of high-harmonic sources with photon energies high enough to access core-to-valence transitions in organic compounds. Core-level absorption spectroscopy is a universal tool that is sensitive to electronic structure, electronic character switching at conical intersections and curve crossings, and nuclear and electronic wave packet dynamics. Amalgamizing the exceptional attosecond time resolution and the sensitivity of X-rays, the attosecond soft X-ray probe is a sought-after utensil offering a richer perspective on complex photochemical questions at the natural timescale of electronic excitation.

Future endeavors in spectroscopic mapping of dynamics through excitations from core to frontier orbitals are envisioned in the direction of separating the symmetry breaking effect from the electronic one in Jahn-Teller systems, and observation of electronic and vibrational coherences with superior time resolution releasing valuable information about non-adiabatic coupling at conical intersections in complex molecular systems.

Acknowledgement

VS and SRL gratefully acknowledge the generous support from the U.S. Department of Energy, Office of Science, Office of Basic Energy Sciences (Contract No. DEAC02-05CH11231), the gas phase chemical physics program as well as the atomic molecular and optical physics program through the Chemical Sciences Division of Lawrence Berkeley National Laboratory, a W.M. Keck Foundation Grant No. 042982, the National Science Foundation (NSF Nos. MRI 1624322, CHE-1951317, and CHE-1660417), the Army Research Office (ARO No. W911NF-14-1-0383), and the Air Force Office of Scientific Research (AFOSR Nos. FA9550-19-1-0314 and FA9550-20-1-0334).

VS acknowledges support from the Swiss National Science Foundation (P2ELP2_184414).

One of the authors (SRL) holds dear his formative years of research with C. Bradley Moore, whose guidance provided valuable insight into being an excellent scientist. A related first article written with by Leone and Moore was a book chapter for volume I, Chemical and Biochemical Applications of Lasers, which served as a model for this contribution by Scutelnic and Leone.

5 Refences

1. Wang, Q., Schoenlein, R., Peteanu, L., Mathies, R. & Shank, C. Vibrationally coherent photochemistry in the femtosecond primary event of vision. *Science* **266**, 422 (1994).
2. Scholes, G. D., Fleming, G. R., Olaya-Castro, A. & van Grondelle, R. Lessons from nature about solar light harvesting. *Nature Chemistry* **3**, 763–774 (2011).
3. Tan, C. *et al.* Direct Determination of Resonance Energy Transfer in Photolyase: Structural Alignment for the Functional State. *J. Phys. Chem. A* **118**, 10522–10530 (2014).
4. Ziemann, P. J. Aerosol products, mechanisms, and kinetics of heterogeneous reactions of ozone with oleic acid in pure and mixed particles. *Faraday Discuss.* **130**, 469–490 (2005).
5. Grosjean, D. Formaldehyde and other carbonyls in Los Angeles ambient air. *Environ. Sci. Technol.* **16**, 254–262 (1982).
6. Yu, G., Gao, J., Hummelen, J. C., Wudl, F. & Heeger, A. J. Polymer Photovoltaic Cells: Enhanced Efficiencies via a Network of Internal Donor-Acceptor Heterojunctions. *Science* **270**, 1789 (1995).
7. Feron, K., Belcher, W. J., Fell, C. J. & Dastoor, P. C. Organic Solar Cells: Understanding the Role of Förster Resonance Energy Transfer. *International Journal of Molecular Sciences* **13**, (2012).
8. Hartridge, H., Roughton, F. J. W. & Langley, J. N. A method of measuring the velocity of very rapid chemical reactions. *Proceedings of the Royal Society of London. Series A, Containing Papers of a Mathematical and Physical Character* **104**, 376–394 (1923).

9. Norrish, R. G. W. & Porter, G. Chemical Reactions Produced by Very High Light Intensities. *Nature* **164**, 658–658 (1949).
10. Eigen, M. & Tamm, K. Schallabsorption in Elektrolytlösungen als Folge chemischer Relaxation I. Relaxationstheorie der mehrstufigen Dissoziation. *Zeitschrift für Elektrochemie, Berichte der Bunsengesellschaft für physikalische Chemie* **66**, 93–107 (1962).
11. Maiman, T. H. Stimulated Optical Radiation in Ruby. *Nature* **187**, 493–494 (1960).
12. McClung, F. J. & Hellwarth, R. W. Giant Optical Pulsations from Ruby. *Journal of Applied Physics* **33**, 828–829 (1962).
13. DeMaria, A. J., Stetser, D. A. & Heynau, H. Self mode-locking of lasers with saturable absorbers. *Appl. Phys. Lett.* **8**, 174–176 (1966).
14. Fork, R. L., Greene, B. I. & Shank, C. V. Generation of optical pulses shorter than 0.1 psec by colliding pulse mode locking. *Appl. Phys. Lett.* **38**, 671–672 (1981).
15. Zewail, A. H. Femtochemistry: Atomic-Scale Dynamics of the Chemical Bond Using Ultrafast Lasers (Nobel Lecture). *Angewandte Chemie International Edition* **39**, 2586–2631 (2000).
16. Mokhtari, A., Cong, P., Herek, J. L. & Zewail, A. H. Direct femtosecond mapping of trajectories in a chemical reaction. *Nature* **348**, 225–227 (1990).
17. Hamm, P., Lim, M., DeGrado, W. F. & Hochstrasser, R. M. The two-dimensional IR nonlinear spectroscopy of a cyclic penta-peptide in relation to its three-dimensional structure. *Proc Natl Acad Sci USA* **96**, 2036 (1999).
18. Repinec, S. T., Sension, R. J. & Hochstrasser, R. M. Femtosecond Studies of the Photoisomerization of cis-Stilbene in Solution. *Berichte der Bunsengesellschaft für physikalische Chemie* **95**, 248–252 (1991).

19. Wang, L., Kohguchi, H. & Suzuki, T. Femtosecond time-resolved photoelectron imaging. *Faraday Discuss.* **113**, 37–46 (1999).
20. Chergui, M. Ultrafast molecular photophysics in the deep-ultraviolet. *J. Chem. Phys.* **150**, 070901 (2019).
21. Fork, R. L., Brito Cruz, C. H., Becker, P. C. & Shank, C. V. Compression of optical pulses to six femtoseconds by using cubic phase compensation. *Opt. Lett.* **12**, 483–485 (1987).
22. Strickland, D. & Mourou, G. Compression of amplified chirped optical pulses. *Optics Communications* **56**, 219–221 (1985).
23. McPherson, A. *et al.* Studies of multiphoton production of vacuum-ultraviolet radiation in the rare gases. *J. Opt. Soc. Am. B* **4**, 595–601 (1987).
24. Lytle, F. The EXAFS family tree: a personal history of the development of extended X-ray absorption fine structure. *Journal of Synchrotron Radiation* **6**, 123–134 (1999).
25. Christian Bressler *et al.* Laser and synchrotron radiation pump-probe x-ray absorption experiment with sub-ns resolution. in vol. 3451 (1998).
26. Chergui, M. & Zewail, A. H. Electron and X-Ray Methods of Ultrafast Structural Dynamics: Advances and Applications. *ChemPhysChem* **10**, 28–43 (2009).
27. Schoenlein, R. W. *et al.* Generation of Femtosecond Pulses of Synchrotron Radiation. *Science* **287**, 2237 (2000).
28. Bostedt, C. *et al.* Linac Coherent Light Source: The first five years. *Rev. Mod. Phys.* **88**, 015007 (2016).
29. Bhattacherjee, A. & Leone, S. R. Ultrafast X-ray Transient Absorption Spectroscopy of Gas-Phase Photochemical Reactions: A New Universal Probe of Photoinduced Molecular Dynamics. *Acc. Chem. Res.* **51**, 3203–3211 (2018).

30. Pertot, Y. *et al.* Time-resolved X-ray absorption spectroscopy with a water window high-harmonic source. *Science* **355**, 264–267 (2017).
31. Schafer, K. J., Yang, B., DiMauro, L. F. & Kulander, K. C. Above threshold ionization beyond the high harmonic cutoff. *Phys. Rev. Lett.* **70**, 1599–1602 (1993).
32. Corkum, P. B. & Krausz, F. Attosecond science. *Nature Physics* **3**, 381–387 (2007).
33. Pfeifer, T. *et al.* Time-resolved spectroscopy of attosecond quantum dynamics. *Chemical Physics Letters* **463**, 11–24 (2008).
34. Krausz, F. & Ivanov, M. Attosecond physics. *Rev. Mod. Phys.* **81**, 163–234 (2009).
35. Goulielmakis, E. *et al.* Real-time observation of valence electron motion. *Nature* **466**, 739–743 (2010).
36. Pollard, W. T. & Mathies, R. A. Analysis of Femtosecond Dynamic Absorption Spectra of Nonstationary States. *Annu. Rev. Phys. Chem.* **43**, 497–523 (1992).
37. Sham, T. K., Yang, B. X., Kirz, J. & Tse, J. S. K-edge near-edge x-ray-absorption fine structure of oxygen- and carbon-containing molecules in the gas phase. *Phys. Rev. A* **40**, 652–669 (1989).
38. Prince, K. C., Richter, R., de Simone, M., Alagia, M. & Coreno, M. Near Edge X-ray Absorption Spectra of Some Small Polyatomic Molecules. *J. Phys. Chem. A* **107**, 1955–1963 (2003).
39. Chang, Z., Corkum, P. B. & Leone, S. R. Attosecond optics and technology: progress to date and future prospects [Invited]. *J. Opt. Soc. Am. B* **33**, 1081–1097 (2016).
40. Timmers, H. *et al.* Polarization-assisted amplitude gating as a route to tunable, high-contrast attosecond pulses. *Optica* **3**, 707–710 (2016).
41. Timmers, H. *et al.* Generating high-contrast, near single-cycle waveforms with third-order dispersion compensation. *Opt. Lett.* **42**, 811–814 (2017).

42. Wheeler, J. A. *et al.* Attosecond lighthouses from plasma mirrors. *Nature Photonics* **6**, 829–833 (2012).

43. Leone, S. R. *et al.* What will it take to observe processes in 'real time'? *Nature Photonics* **8**, 162–166 (2014).

44. Timmers, H. *et al.* Disentangling conical intersection and coherent molecular dynamics in methyl bromide with attosecond transient absorption spectroscopy. *Nature Communications* **10**, 3133 (2019).

45. Wei, Z. *et al.* Elucidating the origins of multimode vibrational coherences of polyatomic molecules induced by intense laser fields. *Nature Communications* **8**, 735 (2017).

46. Kobayashi, Y. *et al.* Coherent electronic-vibrational dynamics in deuterium bromide probed via attosecond transient-absorption spectroscopy. *Phys. Rev. A* **101**, 063414 (2020).

47. Kobayashi, Y., Chang, K. F., Zeng, T., Neumark, D. M. & Leone, S. R. Direct mapping of curve-crossing dynamics in IBr by attosecond transient absorption spectroscopy. *Science* **365**, 79–83 (2019).

48. Ren, X. *et al.* Attosecond light sources in the water window. *Journal of Optics* **20**, 023001 (2018).

49. Attar, A. R. *et al.* Femtosecond x-ray spectroscopy of an electrocyclic ring-opening reaction. *Science* **356**, 54–59 (2017).

50. Epshtein, M. *et al.* Table-Top X-ray Spectroscopy of Benzene Radical Cation. *J. Phys. Chem. A* **124**, 9524–9531 (2020).

51. Vidal, M. L. *et al.* Interplay of Open-Shell Spin-Coupling and Jahn–Teller Distortion in Benzene Radical Cation Probed by X-ray Spectroscopy. *J. Phys. Chem. A* **124**, 9532–9541 (2020).

52. Scutelnic, V. *et al.* X-ray transient absorption reveals the 1Au (nπ*) state of pyrazine in electronic relaxation. *Preprint* (2021).

53. Bhattacherjee, A. & Leone, S. R. Ultrafast X-ray Transient Absorption Spectroscopy of Gas-Phase Photochemical Reactions: A New Universal Probe of Photoinduced Molecular Dynamics. *Acc. Chem. Res.* **51**, 3203–3211 (2018).

54. Li, J. *et al.* 53-attosecond X-ray pulses reach the carbon K-edge. *Nature Communications* **8**, 186 (2017).

55. Gaumnitz, T. *et al.* Streaking of 43-attosecond soft-X-ray pulses generated by a passively CEP-stable mid-infrared driver. *Opt. Express* **25**, 27506–27518 (2017).

56. Pupeikis, J. *et al.* Water window soft X-ray source enabled by a 25 W few-cycle 2.2μm OPCPA at 100 kHz. *Optica* **7**, 168–171 (2020).

57. Johnson, A. S. *et al.* High-flux soft X-ray harmonic generation from ionization-shaped few-cycle laser pulses. *Sci Adv* **4**, eaar3761 (2018).

58. Shiner, A. D. *et al.* Wavelength Scaling of High Harmonic Generation Efficiency. *Phys. Rev. Lett.* **103**, 073902 (2009).

59. Barreau, L. *et al.* Efficient table-top dual-wavelength beamline for ultrafast transient absorption spectroscopy in the soft X-ray region. *Scientific Reports* **10**, 5773 (2020).

60. Kobayashi, Y., Zeng, T., Neumark, D. M. & Leone, S. R. NaI revisited: Theoretical investigation of predissociation via ultrafast XUV transient absorption spectroscopy. *J. Chem. Phys.* **151**, 204103 (2019).

61. Tsuru, S. *et al.* Time-resolved near-edge X-ray absorption fine structure of pyrazine from electronic structure and nuclear wave packet dynamics simulations. *J. Chem. Phys.* **151**, 124114 (2019).

62. Fábri, C., Halász, G. J., Cederbaum, L. S. & Vibók, Á. Signatures of light-induced nonadiabaticity in the field-dressed vibronic spectrum of formaldehyde. *J. Chem. Phys.* **154**, 124308 (2021).
63. Jadoun, D., Gudem, M. & Kowalewski, M. Capturing Fingerprints of Conical Intersection: Complementary Information of Non-Adiabatic Dynamics from Linear X-ray Probes. *Preprint* (2021).
64. Trabattoni, A. *et al.* Charge migration in photo-ionized aromatic amino acids. *Philosophical Transactions of the Royal Society A: Mathematical, Physical and Engineering Sciences* **377**, 20170472 (2019).
65. Chen, M. & Lopata, K. First-Principles Simulations of X-ray Transient Absorption for Probing Attosecond Electron Dynamics. *J. Chem. Theory Comput.* **16**, 4470–4478 (2020).
66. Zinchenko, K. S. *et al.* Sub-7-femtosecond conical-intersection dynamics probed at the carbon K-edge. *Science* **371**, 489 (2021).
67. Lindblad, R. *et al.* X-Ray Absorption Spectrum of the N2+ Molecular Ion. *Phys. Rev. Lett.* **124**, 203001 (2020).
68. Couto, R. C. *et al.* The carbon and oxygen K-edge NEXAFS spectra of CO+. *Phys. Chem. Chem. Phys.* **22**, 16215–16223 (2020).
69. Bari, S. *et al.* Inner-shell X-ray absorption spectra of the cationic series NHy+ (y = 0–3). *Phys. Chem. Chem. Phys.* **21**, 16505–16514 (2019).